RSC Advances

ROYAL SOCIETY OF CHEMISTRY

www.rsc.org/advances

Table of contents entry:

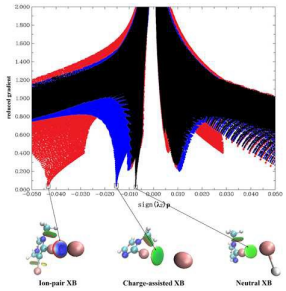

The properties of three different types of halogen bonds in the complexes of imidazolium species are characterized.

RSC Advances

PAPER

Halogen bonding interactions in ion pairs versus conventional charge-assisted and neutral halogen bonds: a theoretical study based on imidazolium species

Received 00th January 20xx,

Accepted 00th January 20xx

DOI: 10.1039/x0xx00000x

www.rsc.org/

Shaozhe Zhang,[a,1] Zhaoqiang Chen,[b,1] Yunxiang Lu,[a,*] Zhijian Xu,[b] Weihong Wu,[a] Weiliang Zhu,[b] Changjun Peng,[a] and Honglai Liu[a]

Halogen bonds in imidazolium-based ion pairs have attracted recent research interest, due to their importance in the fields of anion recognition and ionic liquids. According to our survey of the Cambridge Structural Database (CSD), a number of crystal structures involving these specific halogen bonds were extracted. In this work, three different types of halogen bonding interactions, i.e. ion-pair halogen bonds, charge-assisted and neutral halogen bonds, in a series of dimeric complexes of imidazolium species were systematically studied at the M06-2x and B3LYP levels of theory. Ion-pair halogen bonds, despite considerably stronger in strength, show similar structural and energetic characteristics to common charge-assisted and neutral halogen bonds. To gain a deeper understanding of these interactions, atoms in molecules (AIM), noncovalent interaction index (NCI), and energy decomposition analysis (EDA) calculations were undertaken. Most halogen bonds in imidazolium-based ion pairs have some covalent character, while the other two kinds of halogen bonds are weak electrostatic interactions. The attraction of ion-pair halogen bonds arises dominantly from electrostatic force, while dispersion interaction plays a minor role. These two terms, however, contribute almost equally to the attraction of neutral halogen bonds. In addition to electrostatic attraction, induction interaction, which corresponds to charge transfer and mixing terms, also plays an important role in ion-pair and charge-assisted halogen bonds. The results presented should assist in the development of potent imidazolium-based anion receptors and novel halogenated ionic liquids with promising properties.

1. Introduction

Halogen bonding (XB), a specific noncovalent interaction involving halogen atoms (X = Cl, Br, I) as electrophilic centers, has received widespread interest over the last decades, due to its crucial role in such diverse fields as crystal engineering, supramolecular architecture, and biomolecular design.[1-10] It is well known that covalently bound halogens (even fluorine) show a region of positive electrostatic potential (ESP)[11] at the outmost portion of these atoms along the R−X bonds. Therefore, an electron-rich atom or group prefers to approach the positive cap, giving rise to a linear XB. Politzer et al. have previously developed the σ-hole concept to rationalize the anisotropic ESP distribution of halogens, and moreover they also extended this concept to interpret other peculiar noncovalent interactions, such as chalcogen and pnicogen bonding.[11-16] However, the geometries of XB are not always driven by electrostatics alone.[17, 18]

Of notable attention is the recent applications of XB in solution phase anion recognition.[19-29] The reported receptors based on this interaction exhibit promising properties in both selectivity and efficiency even in competitive polar and polar/aqueous solvents. Particularly, the 2-halo-imidazolium unit, shown in Scheme 1, has been widely employed as a potent binding site for a variety of anions.[23, 25, 29] For example, in 2010 Beer and co-workers demonstrated that the XB (C^2–Br···Cl^-) formation enhances the binding of chloride ion for templated pseudorotaxanes between 2-bromo-imidazolium threading component and an isophthalamide macrocycles, in comparison with hydrogen-bonded (N–H···Cl^-) pseudorotaxane analogues.[23] Subsequently, the group of Metrangolo and Resnati performed a detailed ^{1}H-NMR study of the anion binding properties of the 2-iodo-imidazolium receptor in DMSO, and they found stronger binding for oxoanions over halides because of the remarkably stronger C^2–I···O^- contacts.[25] More recently, the cationic multitopic ligands possessing the 2-iodo-imidazolium unit attached to bipodal and tripodal benzene scaffolds has been explored, and anion binding by these derivatives combines the strength of Coulombic attraction and the directionality of the C^2–I···X^- interactions.[29]

[a]*Key Laboratory for Advanced Materials and Department of Chemistry, East China University of Science and Technology, Shanghai 200237, China. E-mail: yxlu@ecust.edu.cn*
[b]*Drug Discovery and Design Center, Shanghai Institute of Materia Medica, Chinese Academy of Sciences, Shanghai, 201203, China*
†[1] These authors contribute equally to this paper.
† Electronic Supplementary Information (ESI) available: See DOI: 10.1039/x0xx00000x

In recent years, halogenated imidazolium-based ionic liquids (ILs) have been the subject of several experimental and theoretical studies.[30-40] The most striking structural feature of these ILs is the occurrence of XBs between the cations and anions. Mukai and Nishikawa firstly analyzed the crystal structures of 1-propyl- and 1-butyl-3-methyl-4,5-dibromo-imidazolium bromides.[32] The XB ($C^{4,5}$–Br···Br^-) and HB (C^2–H···Br^-) network structures were observed in these crystals, leading to planar-layer motifs with successive honeycomb-like frameworks. Then, they prepared and characterized two halogenated ILs, 4,5-dibromo- and 4,5-diiodo-1-butyl-3-methyl-imidazolium trifluoromethanesulfonates, using differential scanning calorimetry and single-crystal X-ray analysis.[33] The different halogen substituents in the cation strongly influence the melting point, glass transition temperature, and crystal structure of these two ILs, attributed to the different strength and linearity between the $C^{4,5}$–Br···O and $C^{4,5}$–I···O contacts. On the basis of the reported X-ray crystal structures, Lü et al. performed density functional theory (DFT) calculations on the ion pairs for these halogenated ILs and found the formation of XB and HB interactions between the cations and anions.[37, 38] More recently, we have theoretically investigated noncovalent interactions in several halogenated ILs and detected the halogen-bonded ring structures and the conformers with the concurrent XB and HB contacts.[39]

As compared to conventional charge-assisted and neutral XBs, far less theoretical attention has been focused on XBs in ion pairs.[41, 42] Very recently, some halogen-bonded complexes of the 1,3-dimethyl-2-halo-imidazolium cations with halide ions have been examined using the MP2 method, and ion-pair XBs in these systems are characterized by huge binding energies with a high electrostatic contribution.[42] However, several issues of these interactions remain largely elusive to date. What is the nature of these bonds? Can they be recognized as normal XBs? Do they have similar structural and energetic properties to conventional XBs? What is the difference between ion-pair and conventional XB interactions?

Considering the great importance of ion-pair XBs in the fields of anion recognition and ILs, a detailed theoretical study at the DFT (M06-2x and B3LYP) level of theory was undertaken herein. A series of ion-pair halogen-bonded complexes formed between halogenated 1,3-dimethyl-imidazolium cations 1-6 (Fig. 1) and halide anions X^- were considered. For comparison, charge-assisted XBs in the dimers of 1-6 with hydrogen halide HX as well as in the systems of halogenated imidazole molecules **7-12** (Fig. 2) with X^-, together with neutral XBs in the complexes between **7-12** and HX, were also taken into account. To gain a deeper understanding of these interactions, the natural bond order (NBO),[43] atoms in molecules (AIM),[44] noncovalent interaction index (NCI),[45] and energy decomposition analysis (EDA)[46] calculations were performed. In addition, a survey of the Cambridge Structural Database (CSD) was also undertaken to provide some insights into ion-pair XBs in crystals. Here it is worth mentioning that all halogen bonds studied in this work arise basically from the same mechanism with a mix of electrostatic, dispersion and induction nature.

2. Theoretical methods

The geometries of all the complexes under study were fully optimized by means of the M06-2x[47] and B3LYP[48, 49] methods. M06-2x, developed by Zhao and Truhlar, has proved to be reliable in the description of various types of noncovalent interactions,[50-52] while the hybrid B3LYP functional has been widely utilized in the studies of cation-anion interactions in ILs.[34, 39, 53-56] The basis set of Peterson and co-workers, aug-cc-pVDZ-PP,[57] obtained from the EMSL Basis Set Exchange, was used for the I atom. The (-PP) notation indicates that relativistic effective core potentials were employed for the core electrons, that is, $1s^22s^22p^63s^23p^63d^{10}$ for I. For the remaining atoms, the Dunning's augmented double-zeta correlation-consistent basis set, aug-cc-pVDZ,[58] was applied. These basis sets have been commonly used for studying different kinds of XBs with a wide range of strength.[55, 59-62] No symmetry or geometry constraint was imposed during the optimizations. Frequency calculations were performed at the same theoretical levels to ensure that all the structures are genuine minima on the potential energy surface. All of these calculations were carried out with the Gaussian 09 suite of programs.[63]

The NBO analysis was employed by the use of the NBO program implemented in the Gaussian 09 package.[64] The AIM calculations were performed by the AIM 2000 software,[65] using the wave functions generated with M06-2x/cc-pVTZ(-PP). The NCI analysis was undertaken with the Multiwfn program[66] and visualized using the VMD package.[67] The EDA calculations were performed with the SAPT0 method using the PSI4 software.[68]

3. Results

3.1 CSD search

In recent years, several crystal structures of 2-halo- and 4,5-halo-imidazolium cations with certain anions have been reported in the studies of XB-based anion recognition and halogenated ILs.[25, 29, 32, 33, 37-40] To gain some insights into ion-pair XBs in crystals, a survey of the CSD (version 5.36, updates November 2014) was undertaken herein. We only considered crystal structures with no disorder and no errors as well as *R*-factor less than 0.1. The following search criteria were utilized: (1) 2-halo- and 4-halo-/5-halo-imidazolium cations (see Scheme 1) are selected as XB donors and anions as acceptors; (2) the interatomic distances between the donor X atoms in the cations and the acceptor Y atoms (Y = F, Cl, Br, I and O, N, S) in the anions are shorter than the sums of the van der Waals (vdW) radii of these atoms;[69] (3) the interaction angles ∠(C–X···Y) are larger than 150°. As shown in Tables S1 and S2, 85 crystal structures with ion-pair X···Y interactions were extracted from the CSD. In these structures, a variety of anions, such as NO_3^-, PF_6^-, X^-, $CF_3SO_3^-$, and transition metal halides, are presented, but a majority of these structures (approximately 55%) contain halide anions X^-.

The database includes 14% Cl···Y, 53% Br···Y, and 33% I···Y interactions with the average intermolecular distances of 3.19 Å, 3.17 Å, and 3.13 Å, respectively, which are

significantly less than the vdW radius sums of the atoms involved. Particularly, the average interaction angle for all the X···Y bonds retrieved from the CSD amounts to about 170°, thus indicating the good linearity of these interactions in crystals. Note that these geometric features of ion-pair XBs in solid state are well reproduced by present DFT computations on model systems.

3.2 Structures and energetics of different types of XBs

The ESP surfaces for the studied imidazolium species **1-12**, together with the most positive surface ESP ($V_{s,max}$) for halogen atoms, are displayed in Figs. 1 and 2. As expected, $V_{s,max}$ for halogens in the imidazolium cations is calculated to be considerably larger than those in the imidazole molecules; the values of $V_{s,max}$ increase with the enlargement of the size of halogen atoms (I > Br > Cl). For the imidazolium cations **1-6**, the X(C^2) atom exhibit a larger $V_{s,max}$ compared with the X(C^4/C^5) atoms, consistent with the stronger acidity of this halogen atom as revealed previously.[39] However, the two X atoms at the 4 and 5 positions in **10-12** have somewhat different $V_{s,max}$ values; $V_{s,max}$ for the X(C^5) atom is predicted to be much larger than that for X(C^4). This can be ascribed to the stronger electron-withdrawing ability of the NR_2 group bound to the C^5 atom with respect to the N=CR moiety attached to C^4. In the next discussions, we only concentrate on XB interactions involving the X(C^5) atom as donor in the complexes of **10-12**. Note that the magnitude of the σ-hole of halogen atoms does not always correlate with strength of XBs.[70]

The M06-2x optimized structures of the complexes under study are graphically depicted in Fig. 3. The key geometric parameters and the interaction energies for these complexes calculated with the M06-2x and B3LYP methods are summarized in Table 1 and Table S3, respectively. Here it is worth mentioning that the structures for **7**-Cl^- and **10**-Cl^- starting from the halogen-bonded geometry always converge to the HB configurations during the optimizations. As shown in Fig. 3, the chloride anion forms two HBs with the ring H(C^5) and the H atom in the methyl group attached to N^1. This HB structure should be more stable than the XB configuration. However, the XB structure is obtained for **1**-Cl^- and 1-HCl, which can be ascribed to the two methyl moieties bound to N^1 and N^3 that may prevent the anion moving towards H(C^5). From Table 1, it is seen that the intermolecular X···X distances in ion-pair complexes are predicted significantly shorter than those in charge-assisted and neutral dimers, thus indicating much stronger X···X interactions in the former systems. Furthermore, the XB lengths in ion-pair and charge-assisted complexes are much less than the sums of the vdW radii of the atoms involved,[69] while these lengths in neutral dimers are equal to or even slightly longer than the vdW radius sums. In addition, all the X···X interactions in ion-pair dimers are essentially linear (∠(C−X···X) ≈ 180°), whereas XBs in neutral complexes to some extent deviate from the linearity. Generally, the computed intermolecular X···X distances in ion-pair complexes are much shorter than those in crystal structures (ca. 3.2 Å),[32] which can be ascribed to the effects of steric hindrance in crystals. However, the directionality of these interactions observed in crystal structures is reproduced by present calculations. Notably, most of the X···X interactions in the complexes of HX tend to adopt the type II geometry, i.e. ∠(C−X···X) ≈ 180° and ∠(H−X···X) ≈ 90°, which indicates the favorable interaction between the halogen σ-hole along the C−X bonds and the negative ESP region perpendicular to the H−X bonds. In addition, the plots of the interaction energy versus the intermolecular X···X distance are explored for **8**-HBr and **9**-HI and graphically depicted in Fig. S1. It is clear that the curve is very flat near the equilibrium X···X distance.

From Table 1, it is also seen that the computed interaction energies of ion-pair complexes span a range between -69.0 kcal/mol and -88.1 kcal/mol, substantially more negative than those of charge-assisted and neutral systems. Therefore, ion-pair XBs are considerably stronger than charge-assisted and neutral ones, concordant with the much shorter intermolecular distances in ion-pair dimers. As expected, the X(C^2) atom forms stronger X···X interactions with halide ions compared with the X(C^4/C^5) atoms; the interaction energies of neutral complexes are predicted very small in magnitude, varying from -0.3 kcal/mol to -1.5 kcal/mol. Neutral XBs thus are very weak in strength, in good agreement with the much longer intermolecular distances and the deviation from the linearity for these interactions. In addition, the trend of the interaction strength (I···I > Br···Br > Cl···Cl) is observed in all the three types of XBs, consistent with the trend of the reduction of the intermolecular X···X distances with respect to the vdW radii sums. In addition, larger reduction is predicted for ion-pair complexes, while neutral systems exhibit much smaller reduction, in line with the strength trend of the three types of XBs. Particularly, the lengthening of the intermolecular X···X distances with respect to the X−X bond lengths decreases with the strengthening of the X···X interactions, opposite to the tendency of the reduction of these distances. Here it is noteworthy that because of the more negative interaction energies and shorter intermolecular distances, XBs in the complexes of the imidazole molecules with X^- are relatively stronger than those in the systems of the imidazolium cations with HX. Therefore, introducing the anions into the systems should be a more effective tool for strengthening XBs.

For a given XB donor, the strength of X···X interactions decreases in the order $Cl^- > Br^- > I^-$, and the intermolecular X···X distances become gradually longer with the increased size of halide anions ($Cl^- < Br^- < I^-$). This is not surprising, due to the trend of the electron-donating ability of these halide anions ($Cl^- > Br^- > I^-$). These results are in good agreement with previous DFT calculations on the complexes of dihalogen molecules (FI and I_2) with halide anions.[71] However, in the systems of HX with a given XB donor, the X···X interactions show similar strength (HCl ≈ HBr ≈ HI), although the intermolecular X···X distances also elongate with the enlarged atomic size (HCl < HBr < HI). This indicates the similar nucleophilic ability of halogen atoms perpendicular to the H−X bond in the three HX molecules.

Comparison of the data in Tables 1 and S3 reveals that the B3LYP method provides quite similar structural and energetic parameters to those of M06-2x for ion-pair XBs. However, as

compared to M06-2x, the B3LYP method generally gives longer intermolecular separations and less negative interaction energies for charge-assisted XBs. Particularly, most of neutral complexes investigated in this work cannot be obtained at the level of B3LYP. This is not surprising, considering the fact that dispersion plays a minor role in ion-pair XBs but contributes significantly to the stability of neutral XBs (see below). Namely, the B3LYP method, which shows poor description of weak dispersion interactions, performs well on ion-pair XBs. This hybrid functional thus can be a feasible method for studying ion-pair interactions in anion recognition and intermolecular interactions in ILs.

3.3 AIM and NCI analyses

The AIM theory has been widely applied to characterize and quantify a variety of noncovalent interactions,[71-73] such as XB, HB, ion-π and π-π stacking bonds. For each of the X···X interactions in the complexes under study, a bond critical point (BCP) between the donor and the acceptor X atoms has been identified within the AIM analysis, as shown in Fig. S2. The topological parameters (ρ_{BCP} and $\nabla^2\rho_{BCP}$) at the BCPs for the studied systems are listed in Table 2. It is clear that $10^2\rho_{BCP}$ is estimated to vary from 0.505 a.u. to 4.630 a.u. for present X···X interactions, out of the HB range suggested by Koch and Popelier (0.2 au ~ 3.5 au).[74] All the values of $\nabla^2\rho_{BCP}$ are calculated to be positive for charge-assisted and neutral systems, which is indicative of typical closed-shell kind of interactions in these complexes. Table 2 also includes the energetic properties at the BCPs, i.e. local one-electron kinetic energy density G(r), local potential energy density V(r), and the electronic energy density H_{BCP} (kinetic G(r) plus potential V(r) energy density). H is a more sensible and appropriate index than $\nabla^2\rho_b$ to character the nature of noncovalent interactions. The sign of H determines whether the interaction is electrostatic dominant ($H > 0$) or covalent dominant ($H < 0$).[75] As a result of the positive values of H_{BCP}, charge-assisted and neutral XBs belong to weak and electrostatic interactions. However, H_{BCP} is computed to be negative for most of ion-pair XBs, which implies that these interactions are very strong and have some degree of covalent character (shared covalent and electrostatic interactions).

It has been well documented that ρ_{BCP} at the BCPs can be used to determine the strength of noncovalent interactions.[73-75] Not surprisingly, considerably larger ρ_{BCP} is predicted for ion-pair XBs with respect to charge-assisted and neutral ones, consistent with the geometric and energetic results for these bonds (vide supra). The correlations between the interaction energies and the values of ρ_{BCP} are explored for ion-pair complexes as well as for charge-assisted and neutral systems, as displayed in Fig. S3. Note that a poor linear correlation was established for ion-pair complexes ($R^2 = 0.61$).

The NCI index is based on the relationship between the electron density ρ(r) and the reduced density gradient s, which is expressed as:

$$s = \frac{1}{2(3\pi^2)^{1/3}} \frac{|\nabla\rho|}{\rho^{4/3}} \quad (1)$$

It allows isosurfaces of the reduced density gradient at low densities to visualize the position and nature of noncovalent interactions in 3D space.[76] This method has been recently used to study various noncovalent interactions, because it can overcome some limitations of the AIM theory and hence provides a more global description of noncovalent bonding.[77] The NCI isosurfaces of three representative complexes, **5**-Br$^-$, **8**-Br$^-$ and **8**-HBr, are depicted in Fig. 4, where strong attractive interactions are represented in blue, weak interactions in green, and repulsive interactions in red. These images clearly indicate typical Br···Br interactions with different strength in the three complexes. The blue isosurface between the donor and acceptor Br atoms in **5**-Br$^-$ corresponds to a strong XB interaction, while the weak Br···Br interactions in **8**-Br$^-$ and **8**-HBr are evident from the green isosurfaces between the two Br atoms.

The plots of s versus the sign of second eigenvalue λ_2 for the three systems are also shown in Fig. 4. The presence of noncovalent interactions is characterized by spikes at negative sign of λ_2, whereas the peaks at positive sign indicate the repulsive steric interactions due to ring formation. Evidently, two main low-gradient spikes are located at negative sign of λ_2 in the plot of **5**-Br$^-$: the first spike at more negative value (about -0.043) indicates the Br···Br interaction, and the second spike corresponds to intramolecular Br···H interactions in the cation. However, BCPs are absent between these two atoms within the AIM analysis (see Fig. S2). The plot of **8**-Br$^-$ is somewhat similar to that of **5**-Br$^-$, except that the first spike resides at considerably less negative value (ca. -0.015). However, in the plot of **8**-HBr the first spike indicates intramolecular Br···H interaction, while the second spike corresponds to the Br···Br interaction (about -0.008), contrary to that in **5**-Br$^-$ and **8**-Br$^-$. This implies very weak XBs in neutral systems, in good agreement with the geometric, energetic and AIM findings as demonstrated above.

3.4 EDA calculations

According to the SAPT0 method,[68] the total interaction energy (ΔE_{int}) can be decomposed into the following four terms:

$$\Delta E_{int} = E_{es} + E_{ex} + E_{ind} + E_{disp} \quad (2)$$

where E_{es} is the electrostatic term describing the classical Coulomb interaction; E_{ind}, which corresponds to the orbital energy including charge transfer and mixing terms, represents the induction energy; E_{disp} is the dispersion term and E_{ex} is the repulsive exchange energy resulting from the Pauli exclusion principle. The total interaction energies and the four components for eight brominated complexes are given in Table 3. Here it is important to note that the total interaction energies calculated with the SAPT0 method correlate excellently well with those of M06-2x/aug-cc-pVDZ ($R^2 = 1$).

For ion-pair XBs, the electrostatic energy is the dominant contribution to the attraction (approximately 70%), while the dispersion term appears to be very small (about 6%). Furthermore, the induction energy provides approximately 23% attraction in these interactions. This indicates that charge transfer and orbital interactions play an important role in these bonds, in good agreement with the results of the NBO analysis (vide infra). Notably, the exchange-repulsion term is

significantly larger in ion-pair XBs, attributed to the much shorter intermolecular separation for these bonds. However, this repulsion energy is much lower than the magnitude of the electrostatic attraction, opposite to that in charge-assisted and neutral XBs, which further suggests the dominant role of electrostatics in ion-pair XBs.

Although the electrostatic energy is still the main attractive term (about 45%) in charge-assisted XBs, the dispersion and induction contributions are also important. Here it is worth noting that as compared to **8**-Br^- and **11**-Br^-, the dispersion energy plays a larger role in the attraction of Br···Br interactions in **2**-HBr and **5**-HBr, whereas the contribution from the electrostatic energy becomes smaller. This is not surprising, considering the much weaker Br···Br interactions in **2**-HBr and **5**-HBr than those in **8**-Br^- and **11**-Br^-. In addition, the induction energy contributes to the attraction of the interactions in **8**-Br^- and **11**-Br^- to a larger degree, in accordance with the larger magnitude of charge transfer and greater values of E^2 for these two complexes (see Table 4).

For neutral XB interactions, the dispersion energy is the largest contribution to the attraction (ca. 48%) and the electrostatic energy is the second contribution (about 40%), while the induction contribution is quite small (about 10%). Considering the strong dispersion component, great care should be taken when choosing theoretical methods to treat these interactions. As mentioned above, the B3LYP method performs poorly on neutral XBs, due to the lack of dispersion energy. On the other hand, this method provides structural and energetic results of ion-pair systems comparable to those of M06-2x, because dispersion plays a minor role in ion-pair XBs.

Recently, Stone has utilized the SAPT(DFT) method to explore the nature of XB interactions in the complexes of dihalogen molecules (ClF, Cl_2 and F_2) with several electron donors, such as NH_3, H_2O, H_2CO, ethyne and ethene.[17] They found that albeit the main contribution to the binding is usually the electrostatic term, the strong tendency to the linearity of these bonds is due to exchange-repulsion, not electrostatics. Then, Huber and co-workers performed EDA calculations on six halogen-bonded complexes of CF_3I, C_6F_5I and I_2 with Cl^- and NH_3 and revealed similar results, that is, the directionality of XB is driven by the synergy between charge-transfer interactions and Pauli repulsion.[18] Therefore, the linearity of XBs in present complexes of imidazolium molecules is not always determined by electrostatics alone.

Overall, strong ion-pair XBs are dominantly electrostatic interactions with a remarkable contribution from induction; weak neutral XBs depend strongly on both dispersion and electrostatics; median strong charge-assisted XBs are mixed electrostatic-induction-dispersion nature. Namely, when the strength of XB increases, the contribution from the dispersion term becomes smaller and the role of electrostatic attraction appears to be more important.

3.5 NBO analysis

The NBO analysis has been recognized as a useful tool in the rationalization of noncovalent interactions. The amount of charge transfer (Q_{CT}), Wiberg bond orders (BO), and the second-order stabilization energies (E^2) due to the LP(X)→σ*(C−X) orbital interactions calculated with the NBO scheme for all the studied complexes are listed in Table 4. As anticipated, a substantial magnitude of charge transfer, ranging from 141 *me* to 463 *me*, occurs in ion-pair complexes; bond orders of ion-pair XBs are computed generally greater than those of charge-assisted and neutral ones. Additionally, for ion-pair XBs the orbital interaction between lone pair of X and σ* of the C−X bond can be viewed as a significant stabilizing interaction, because of the large values of E^2 (19.87-88.29 kcal/mol). This agrees well with the EDA results that the induction term, which includes the charge transfer contribution, play an important role in the attraction of ion-pair XB interactions (see above).

4. Discussion

According to our calculations, ion-pair XBs in the complexes of imidazolium species are characterized by a huge binding energy and hence are considerably stronger than traditional charge-assisted and neutral ones. These peculiar interactions show some character of covalency, on the basis of the AIM and NCI analyses. The electrostatic term is the dominant contribution (70%) to the attraction in ion-pair XBs, while the dispersion contribution is very small (6%). Charge transfer and orbital interactions, which are related to the induction term, also play an important role in these bonds. However, ion-pair XBs exhibit some geometric and energetic features similar to conventional charge-assisted and neutral XBs, such as the directionality and the strength trend (I > Br > Cl).

In previous studies of XB-based anion recognition,[25, 29] the 2-iodo-imidazolium unit was commonly used in the design of potent anion receptors. Our calculations revealed that the 2-iodo-imidazolium cation forms much stronger ion-pair XBs with halide anions, as compared to the 2-chloro/2-bromo-imidazolium and 4-halo/5-halo-imidazolium counterparts. Consequently, the receptors based on this unit can strongly bind various anions and show selectivity for the anions. However, ion-pair XBs in the complexes of the latter cations are still very strong and also exhibit similar characteristics to those involving the 2-iodo-imidazolium cation. These units thus can be employed in anion recognition for some particular purposes, such as special macrocycles and bipodal/tripodal scaffolds, unique selectivity for certain anions, and multi-donor center receptors. For example, the bis-2-halo-imidazolim macrocycles have been recently employed in XB-based anion recognition,[27] because the two X(C^2) atoms simultaneously interact with the anion through short XB contacts. When halogen substituents are introduced into the 4,5 positions (4,5-dihalo-imidazolium units) in the macrocycles, four X(C^4/C^5) atoms (multidentate donor center) can form strong XBs with the anion, which may enhance the efficiency. Additionally, the smaller size of the Cl and Br atoms can also be utilized in anion receptor design in terms of spatial effects.

Recently, Mukai and Nishikawa have synthesized and characterized four halogenated ILs involving the 4,5-dibromo- and 4,5-diiodo-imidazolium cations.[33, 40] They found that the

introduction of the halogen substitution at the 4 and 5 positions results in a higher melting temperature than the non-halogenated IL, due to the increased intermolecular interaction energy.[33] In the light of present calculations, the X(C^2) atom shows a larger value of $V_{s,max}$ than the X(C^4/C^5) atoms and hence XBs in the systems of the 2-halo-imidazolium cation become somewhat stronger than those in the complexes of the 4,5-dihalo-imidazolium analogues. The 2-halo-imidazolium unit, accordingly, is not a good scaffold for the development of room temperature ILs. Notably, the strength of ion-pair XBs tends to increase with the enlargement of the atomic radius of halogens (I > Br > Cl), which agrees well with the experimental findings that the iodinated IL exhibits a higher melting temperature than the corresponding brominated IL (125.0 °C vs 73.2 °C).[33] On the basis of these, the ILs containing the 4,5-dichloro-imidazolium cation may possess a low melting temperature due to the decreased intermolecular interaction energy and thus can be employed for further exploration.

In summary, the 2-chloro-/2-bromo- and 4-halo-/5-halo-imidazolium units can be employed in the design of XB-based anion receptors, although the 2-iodo-imidazolium unit has been frequently used in previous attempts. The 4,5-dichloro-imidazolium unit could be a better scaffold for developing ILs with promising properties, owing to the weaker intermolecular interactions. Additionally, both the computations and the CSD search revealed the linearity of ion-pair XBs, which may be very useful in the design of novel anion receptors and functional ILs.

5. Conclusions

The main conclusions of the present work are summarized as follows:

1. Ion-pair XBs are characterized by large binding energies and have some degree of covalent nature.

2. The electrostatic term play a dominant role in the attraction of ion-pair XBs, while the dispersion contribution is very small. The induction term, which corresponds to charge transfer and mixing interactions, also contributes significantly to the stability of these interactions.

3. As a result of the strong dispersion component in neutral XBs, DFT methods including the dispersion correction should be necessary for treating these interactions. The B3LYP method, which provides poor performance on weak neutral XBs, can be employed in the studies of ion-pair interactions in anion recognition and intermolecular interactions in ILs.

4. In addition to the 2-iodo-imidazoliom cation, the 2-chloro/2-bromo- and 4-halo-/5-halo-imidazolium units should also be good candidates for developing potent anion receptors. The 4,5-dichloro-imidazolium cation could be a better scaffold in the design of novel halogenated ILs exhibiting promising properties.

We hope that the results reported in this work will assist in the design of efficient anion receptors and novel functional ILs based on the halogenated imidazolium units.

Acknowledgements

This work was supported by the National Key Basic Research Program of China (2015CB251401), the National Natural Science Foundation of China (21473054), and the Fundamental Research Funds of the Central Universities of China (222201313001).

Notes and References

1. R. B. Walsh, C. W. Padgett, P. Metrangolo, G. Resnati, T. Hanks and W. T. Pennington, *Cryst. Growth Des.*, 2001, **1**, 165-175.
2. B. K. Saha, A. Nangia and M. Jaskólski, *CrystEngComm*, 2005, **7**, 355-358.
3. P. Metrangolo, G. Resnati, T. Pilati and S. Biella, in *Halogen Bonding*, Springer, 2008, pp. 105-136.
4. A. Mukherjee, S. Tothadi and G. R. Desiraju, *Acc. Chem. Res.*, 2014, **47**, 2514-2524.
5. P. Metrangolo and G. Resnati, *Chem. Eur. J.*, 2001, **7**, 2511-2519.
6. P. Metrangolo, F. Meyer, T. Pilati, G. Resnati and G. Terraneo, *Angew. Chem. Int. Ed.*, 2008, **47**, 6114-6127.
7. A. Priimagi, G. Cavallo, P. Metrangolo and G. Resnati, *Acc. Chem. Res.*, 2013, **46**, 2686-2695.
8. P. Auffinger, F. A. Hays, E. Westhof and P. S. Ho, *Proc Natl Acad Sci U S A*, 2004, **101**, 16789-16794.
9. Y. Lu, Y. Wang and W. Zhu, *Phys. Chem. Chem. Phys.*, 2010, **12**, 4543-4551.
10. Y. Lu, Y. Liu, Z. Xu, H. Li, H. Liu and W. Zhu, *Exp. Op. Drug Disc.*, 2012, **7**, 375-383.
11. T. Clark, M. Hennemann, J. S. Murray and P. Politzer, *J. Mol. Model.*, 2007, **13**, 291-296.
12. A. Bauzá, I. Alkorta, A. Frontera and J. Elguero, *J. Chem. Theory Comput.*, 2013, **9**, 5201-5210.
13. P. Politzer, J. S. Murray and T. Clark, *Phys. Chem. Chem. Phys.*, 2010, **12**, 7748-7757.
14. P. Politzer, K. E. Riley, F. A. Bulat and J. S. Murray, *Comput. Theor. Chem.*, 2012, **998**, 2-8.
15. P. Politzer, J. S. Murray and T. Clark, *Phys. Chem. Chem. Phys.*, 2013, **15**, 11178-11189.
16. P. Politzer and J. S. Murray, in *Noncovalent Forces*, Springer, 2015, pp. 291-321.
17. A. J. Stone, *J. Am. Chem. Soc.*, 2013, **135**, 7005-7009.
18. S. M. Huber, J. D. Scanlon, E. Jimenez-Izal, J. M. Ugalde and I. Infante, *Phys. Chem. Chem. Phys.*, 2013, **15**, 10350-10357.
19. P. Metrangolo, H. Neukirch, T. Pilati and G. Resnati, *Acc. Chem. Res.*, 2005, **38**, 386-395.
20. P. Metrangolo, T. Pilati, G. Terraneo, S. Biella and G. Resnati, *CrystEngComm*, 2009, **11**, 1187-1196.
21. E. Dimitrijević, O. Kvak and M. S. Taylor, *Chem. Commun.*, 2010, **46**, 9025-9027.
22. G. Cavallo, P. Metrangolo, T. Pilati, G. Resnati, M. Sansotera and G. Terraneo, *Chem. Soc. Rev.*, 2010, **39**, 3772-3783.
23. C. J. Serpell, N. L. Kilah, P. J. Costa, V. Félix and P. D.

Beer, *Angew. Chem. Int. Ed.*, 2010, **49**, 5322-5326.
24. N. L. Kilah, M. D. Wise and P. D. Beer, *Cryst. Growth Des.*, 2011, **11**, 4565-4571.
25. M. Cametti, K. Raatikainen, P. Metrangolo, T. Pilati, G. Terraneo and G. Resnati, *Org. Biomol. Chem.*, 2012, **10**, 1329-1333.
26. F. Kniep, L. Rout, S. M. Walter, H. K. Bensch, S. H. Jungbauer, E. Herdtweck and S. M. Huber, *Chem. Commun.*, 2012, **48**, 9299-9301.
27. F. Zapata, A. Caballero, N. G. White, T. D. Claridge, P. J. Costa, V. Felix and P. D. Beer, *J. Am. Chem. Soc.*, 2012, **134**, 11533-11541.
28. S. M. Walter, F. Kniep, L. Rout, F. P. Schmidtchen, E. Herdtweck and S. M. Huber, *J. Am. Chem. Soc.*, 2012, **134**, 8507-8512.
29. K. Raatikainen, G. Cavallo, P. Metrangolo, G. Resnati, K. Rissanen and G. Terraneo, *Cryst. Growth Des.*, 2013, **13**, 871-877.
30. J. Jacquemin, P. Husson, V. Mayer and I. Cibulka, *J. Chem. Eng. Data*, 2007, **52**, 2204-2211.
31. D. Kerlé, R. Ludwig, A. Geiger and D. Paschek, *J. Phys. Chem. B*, 2009, **113**, 12727-12735.
32. T. Mukai and K. Nishikawa, *Chem. Lett.*, 2009, **38**, 402-403.
33. T. Mukai and K. Nishikawa, *Solid State Sci*, 2010, **12**, 783-788.
34. A. M. Fernandes, M. A. Rocha, M. G. Freire, I. M. Marrucho, J. A. Coutinho and L. M. Santos, *J. Phys. Chem. B*, 2011, **115**, 4033-4041.
35. Y. Deng, P. Besse-Hoggan, M. Sancelme, A. M. Delort, P. Husson and M. F. Gomes, *J. Hazard. Mater.*, 2011, **198**, 165-174.
36. C. Han, G. G. Yu, L. Wen, D. C. Zhao, C. Asumana and X. C. Chen, *Fluid Phase Equilib.*, 2011, **300**, 95-104.
37. R. Lü, S. Wang and Y. Lu, *Chem. Phys. Lett.*, 2011, **505**, 87-91.
38. R. Lü, Z. Qu, H. Yu, F. Wang and S. Wang, *Comput. Theor. Chem.*, 2012, **988**, 86-91.
39. H. Li, Y. Lu, W. Wu, Y. Liu, C. Peng, H. Liu and W. Zhu, *Phys. Chem. Chem. Phys.*, 2013, **15**, 4405-4414.
40. T. Mukai and K. Nishikawa, *Rsc. Adv.*, 2013, **3**, 19952-19955.
41. J. E. Del Bene, I. Alkorta and J. Elguero, *J. Phys. Chem. A*, 2010, **114**, 12958-12962.
42. O. Donoso-Tauda, P. Jaque, J. Elguero and I. Alkorta, *J. Phys. Chem. A*, 2014, **118**, 9552-9560.
43. A. E. Reed, L. A. Curtiss and F. Weinhold, *Chem. Rev.*, 1988, **88**, 899-926.
44. R. F. Bader, *Atoms in molecules*, Wiley Online Library, 1990.
45. E. R. Johnson, S. Keinan, P. Mori-Sanchez, J. Contreras-Garcia, A. J. Cohen and W. Yang, *J. Am. Chem. Soc.*, 2010, **132**, 6498-6506.
46. K. Kitaura and K. Morokuma, *Int. J. Quantum Chem*, 1976, **10**, 325-340.
47. Y. Zhao and D. G. Truhlar, *Theor. Chem. Acc.*, 2008, **120**, 215-241.
48. A. D. Becke, *Phys. Rev. A*, 1988, **38**, 3098-3100.
49. C. Lee, W. Yang and R. G. Parr, *Phys. Rev. B*, 1988, **37**, 785-789.
50. Y. Zhao and D. G. Truhlar, *J. Chem. Theory Comput.*, 2008, **4**, 1849-1868.
51. Y. Zhao and D. G. Truhlar, *Acc. Chem. Res.*, 2008, **41**, 157-167.
52. L. P. Wolters, P. Schyman, M. J. Pavan, W. L. Jorgensen, F. M. Bickelhaupt and S. Kozuch, *WIREs Comput. Mol. Sci.*, 2014, **4**, 523–540.
53. P. A. Hunt, B. Kirchner and T. Welton, *Chem. Eur. J.*, 2006, **12**, 6762-6775.
54. H. Niedermeyer, M. A. Ab Rani, P. D. Lickiss, J. P. Hallett, T. Welton, A. J. White and P. A. Hunt, *Phys. Chem. Chem. Phys.*, 2010, **12**, 2018-2029.
55. X. Zhu, Y. Lu, C. Peng, J. Hu, H. Liu and Y. Hu, *J. Phys. Chem. B*, 2011, **115**, 3949-3958.
56. W. Wu, Y. Lu, H. Ding, C. Peng and H. Liu, *Phys. Chem. Chem. Phys.*, 2015, **17**, 1339-1346.
57. K. A. Peterson, D. Figgen, E. Goll, H. Stoll and M. Dolg, *J. Chem. Phys*, 2003, **119**, 11113-11123.
58. R. A. Kendall, T. H. Dunning Jr and R. J. Harrison, *J. Chem. Phys.*, 1992, **96**, 6796-6806.
59. H. Ding, Y. Lu, W. Wu and H. Liu, *Chem. Phys.*, 2014, **441**, 30-37.
60. Y. X. Lu, J. W. Zou, Y. H. Wang, Y. J. Jiang and Q. S. Yu, *J. Phys. Chem. A*, 2007, **111**, 10781-10788.
61. Y. Lu, H. Li, X. Zhu, W. Zhu and H. Liu, *J. Phys. Chem. A*, 2011, **115**, 4467-4475.
62. Y. Lu, Y. Liu, H. Li, X. Zhu, H. Liu and W. Zhu, *J. Phys. Chem. A*, 2012, **116**, 2591-2597.
63. R. A. Gaussian 09, M. J. Frisch, G. W. Trucks, H. B. Schlegel, G. E. Scuseria, M. A. Robb, J. R. Cheeseman, G. Scalmani, V. Barone, B. Mennucci, G. A. Petersson, H. Nakatsuji, M. Caricato, X. Li, H. P. Hratchian, A. F. Izmaylov, J. Bloino, G. Zheng, J. L. Sonnenberg, M. Hada, M. Ehara, K. Toyota, R. Fukuda, J. Hasegawa, M. Ishida, T. Nakajima, Y. Honda, O. Kitao, H. Nakai, T. Vreven, J. A. Montgomery, Jr., J. E. Peralta, F. Ogliaro, M. Bearpark, J. J. Heyd, E. Brothers, K. N. Kudin, V. N. Staroverov, R. Kobayashi, J. Normand, K. Raghavachari, A. Rendell, J. C. Burant, S. S. Iyengar, J. Tomasi, M. Cossi, N. Rega, J. M. Millam, M. Klene, J. E. Knox, J. B. Cross, V. Bakken, C. Adamo, J. Jaramillo, R. Gomperts, R. E. Stratmann, O. Yazyev, A. J. Austin, R. Cammi, C. Pomelli, J. W. Ochterski, R. L. Martin, K. Morokuma, V. G. Zakrzewski, G. A. Voth, P. Salvador, J. J. Dannenberg, S. Dapprich, A. D. Daniels, O. Farkas, J. B. Foresman, J. V. Ortiz, J. Cioslowski, and D. J. Fox, Gaussian, Inc., Wallingford CT, 2009.
64. E. D. Glendening, C. R. Landis and F. Weinhold, *J. Comput. Chem.*, 2013, **34**, 1429-1437.
65. F. Biegler-König, J. Schönbohm and D. Bayles, *J. Comput. Chem.*, 2001, **22**, 545-559.
66. T. Lu and F. Chen, *J. Comput. Chem.*, 2012, **33**, 580-592.
67. W. Humphrey, A. Dalke and K. Schulten, *J. Mol. Graphics*, 1996, **14**, 33-38, 27-38.

68. J. M. Turney, A. C. Simmonett, R. M. Parrish, E. G. Hohenstein, F. A. Evangelista, J. T. Fermann, B. J. Mintz, L. A. Burns, J. J. Wilke and M. L. Abrams, *WIREs. Comput. Mol. Sci.*, 2012, **2**, 556-565.
69. A. Bondi, *J. Phys. Chem.*, 1964, **68**, 441-451.
70. S. M. Huber, E. Jimenez-Izal, J. M. Ugalde and I. Infante, *Chem. Commun.*, 2012, **48**, 7708-7710.
71. D. Quiñonero, A. Frontera, C. Garau, P. Ballester, A. Costa and P. M. Deyà, *ChemPhysChem*, 2006, **7**, 2487-2491.
72. U. Koch and P. Popelier, *J. Phys. Chem.*, 1995, **99**, 9747-9754.
73. J. W. Zou, Y. X. Lu, Q. S. Yu, H. X. Zhang and Y. J. Jiang, *Chin. J. Chem* . 2006, **24**, 1709-1715.
74. P. Popelier, *J. Phys. Chem. A*, 1998, **102**, 1873-1878.
75. I. Alkorta, I. Rozas and J. Elguero, *J. Phys. Chem. A*, 1998, **102**, 9278-9285.
76. J. Contreras-Garcia, E. R. Johnson, S. Keinan, R. Chaudret, J. P. Piquemal, D. N. Beratan and W. Yang, *J. Chem. Theory Comput.*, 2011, **7**, 625-632.
77. J. R. Lane, J. Contreras-García, J.-P. Piquemal, B. J. Miller and H. G. Kjaergaard, *J. Chem. Theory Comput.*, 2013, **9**, 3263-3266.

Table 1. Geometric and energetic data calculated with M06-2x for all the studied complexes[a]

	ΔE	d(X···X)	Reduction (%) of vdW radii sum	∠(C-X···X)
Ion-pair complexes				
1-Cl$^-$	-76.5	2.653	24.2	178.1
2-Cl$^-$	-85.2	2.564	29.2	179.6
2-Br$^-$	-80.7	2.731	27.0	179.8
2-I$^-$	-76.3	2.932	25.0	179.6
3-I$^-$	-88.1	2.955	27.6	179.8
4-Cl$^-$	-69.0	2.697	22.9	173.9
5-Cl$^-$	-76.9	2.592	28.4	177.3
5-Br$^-$	-72.7	2.763	26.1	177.1
5-I$^-$	-68.6	2.970	24.0	176.8
6-I$^-$	-78.9	2.989	26.7	179.1
Charge-assisted complexes				
1-HCl	-2.7	3.313	5.3	167.0
2-HCl	-3.5	3.277	9.5	175.2
2-HBr	-3.5	3.405	8.9	173.7
2-HI	-3.4	3.601	7.9	178.1
3-HI	-5.0	3.628	11.1	177.1
4-HCl	-2.4	3.339	4.6	167.3
5-HCl	-3.0	3.306	8.7	174.9
5-HBr	-3.0	3.431	8.2	177.3
5-HI	-3.0	3.629	7.2	175.6
6-HI	-4.2	3.661	10.3	178.6
7-Cl$^-$	---	---	---	---
8-Cl$^-$	-9.2	3.057	15.6	172.4
8-Br$^-$	-7.8	3.268	12.6	170.4
8-I$^-$	-6.4	3.534	9.6	166.9
9-I$^-$	-11.5	3.449	15.5	175.8
10-Cl$^-$	---	---	---	---
11-Cl$^-$	-13.0	2.986	17.5	173.0
11-Br$^-$	-11.3	3.201	14.4	170.9
11-I$^-$	-9.5	3.462	11.5	168.4
12-I$^-$	-15.4	3.362	17.6	176.2
Neutral complexes				
7-HCl	-0.3	3.564	-1.8	136.1
8-HCl	-0.9	3.527	2.6	167.7
8-HBr	-1.3	3.635	2.8	175.5
8-HI	-1.1	3.797	2.9	176.9
9-HI	-1.5	3.903	4.3	168.4
10-HCl	-0.4	3.513	-0.4	167.2
11-HCl	-0.9	3.505	3.2	165.5
11-HBr	-1.3	3.615	3.3	176.1
11-HI	-1.1	3.757	3.9	158.9
12-HI	-1.5	3.880	4.4	164.7

[a] Energies are given in kcal/mol, distances in angstroms, and angles in degrees. The complexes **7**-Cl$^-$ and **10**-Cl$^-$ cannot be obtained at the level of M06-2x/aug-cc-pVDZ.

Table 2. The AIM data calculated with M06-2x for all the studied complexes[a]

	$10^2\rho_{BCP}$	$10^2\nabla^2\rho_{BCP}$	10^2V_{BCP}	10^2G_{BCP}	10^2H_{BCP}
Ion-pair complexes					
1-Cl$^-$	3.748	10.618	-2.511	2.583	0.072
2-Cl$^-$	5.409	9.846	-3.864	3.163	-0.701
2-Br$^-$	4.63	7.625	-2.879	2.393	-0.487
2-I$^-$	4.044	5.329	-2.219	1.776	-0.444
3-I$^-$	4.584	4.058	-2.701	1.858	-0.843
4-Cl$^-$	3.382	10.063	-2.219	2.367	0.148
5-Cl$^-$	5.104	9.707	-3.573	3.000	-0.573
5-Br$^-$	4.346	7.524	-2.655	2.268	-0.387
5-I$^-$	3.747	5.343	-2.020	1.678	-0.342
6-I$^-$	4.293	4.254	-2.481	1.772	-0.709

Charge-assisted complexes					
1-HCl	0.862	3.017	-0.458	0.606	0.148
2-HCl	1.120	3.757	-0.598	0.769	0.171
2-HBr	1.102	3.313	-0.553	0.691	0.138
2-HI	1.031	2.782	-0.456	0.576	0.120
3-HI	1.189	3.017	-0.528	0.641	0.113
4-HCl	0.824	2.869	-0.436	0.577	0.140
5-HCl	1.058	3.544	-0.564	0.725	0.161
5-HBr	1.059	3.173	-0.533	0.663	0.130
5-HI	0.972	2.652	-0.432	0.548	0.115
6-HI	1.117	2.886	-0.496	0.609	0.113
7-Cl^-	---	---	---	---	---
8-Cl^-	1.870	5.790	-1.055	1.251	0.196
8-Br^-	1.532	4.270	-0.779	0.923	0.144
8-I^-	1.225	3.113	-0.546	0.662	0.116
9-I^-	1.736	3.778	-0.811	0.878	0.067
10-Cl^-	---	---	---	---	---
11-Cl^-	2.152	6.530	-1.249	1.441	0.192
11-Br^-	1.738	4.777	-0.903	1.049	0.146
11-I^-	1.389	3.491	-0.634	0.754	0.119
12-I^-	2.049	4.131	-0.989	1.011	0.022
Neutral complexes					
7-HCl	0.505	1.705	-0.259	0.343	0.083
8-HCl	0.693	2.222	-0.352	0.454	0.102
8-HBr	0.734	2.154	-0.360	0.449	0.089
8-HI	0.715	1.978	-0.316	0.405	0.089
9-HI	0.717	1.924	-0.298	0.390	0.091
10-HCl	0.542	1.877	-0.283	0.376	0.093
11-HCl	0.699	2.286	-0.358	0.465	0.107
11-HBr	0.754	2.234	-0.372	0.465	0.093
11-HI	0.733	2.044	-0.328	0.419	0.092
12-HI	0.749	2.012	-0.313	0.408	0.095

[a] All values are given in a.u.

Table 3. The total interaction energy ΔE_{int} and its contributions for eight brominated complexes[a]

	ΔE_{int}	E_{es}	E_{ex}	E_{ind}	E_{disp}
Ion-pair complexes					
2-Br^-	-81.20	-101.13(70.4%)	62.44	-33.39(23.2%)	-9.12(6.3%)
5-Br^-	-71.27	-90.53(70.3%)	57.53	-29.50(22.9%)	-8.78(6.8%)
Charge-assisted complexes					
2-HBr	-3.30	-3.85(44.8%)	5.30	-2.18(25.4%)	-2.56(29.8%)
5-HBr	-2.73	-3.48(44.8%)	5.03	-1.75(22.6%)	-2.53(32.6%)
8-Br^-	-7.62	-10.30(45.5%)	14.99	-8.14(36.0%)	-4.18(18.5%)
11-Br^-	-10.48	-14.18(50.1%)	17.85	-9.51(33.6%)	-4.64(16.4%)
Neutral complexes					
8-HBr	-1.17	-1.62(41.0%)	2.77	-0.43(10.9%)	-1.90(48.1%)
11-HBr	-1.14	-1.57(39.1%)	2.89	-0.48(11.9%)	-1.97(49.0%)

[a] All values are given in kcal/mol. The values in parentheses are the corresponding percentages of the three energy terms in the attraction.

Table 4. The amount of charge transfer (Q_{CT}), Wiberg bond orders (BO), and second-order perturbation energies (E^2) of LP(X)→BD*(C–X) for all the studied complexes[a]

	Q_{CT}	Wiberg BO	E^2
Ion-pair complexes			
1-Cl^-	-0.161	0.169	23.3
2-Cl^-	-0.305	0.324	61.3
2-Br^-	-0.311	0.323	55.1
2-I^-	-0.342	0.345	52.6
3-I^-	-0.463	0.497	88.3
4-Cl^-	-0.141	0.150	19.9
5-Cl^-	-0.286	0.002	56.1
5-Br^-	-0.287	0.309	49.6
5-I^-	-0.307	0.003	45.1
6-I^-	-0.422	0.464	75.1
Charge-assisted complexes			
1-HCl	-0.007	0.008	1.3
2-HCl	-0.016	0.019	3.6
2-HBr	-0.020	0.024	3.8
2-HI	-0.027	0.032	4.0
3-HI	-0.050	0.064	7.4
4-HCl	-0.006	0.007	1.2
5-HCl	-0.014	0.017	3.2
5-HBr	-0.018	0.022	3.6
5-HI	-0.022	0.027	3.6
6-HI	-0.042	0.056	6.5
7-Cl^-	---	---	---
8-Cl^-	-0.063	0.070	9.9
8-Br^-	-0.054	0.059	7.8
8-I^-	-0.046	0.050	5.9
9-I^-	-0.112	0.132	14.2
10-Cl^-	---	---	---
11-Cl^-	-0.080	0.090	12.8
11-Br^-	-0.068	0.077	10.0
11-I^-	-0.059	0.066	7.7
12-I^-	-0.145	0.172	18.9
Neutral complexes			
7-HCl	-0.001	0.004	0.1

8-HCl	-0.004	0.006	1.2
8-HBr	-0.006	0.008	1.6
8-HI	-0.007	0.010	1.8
9-HI	-0.010	0.016	2.5
10-HCl	-0.001	0.004	0.3
11-HCl	-0.004	0.006	1.2
11-HBr	-0.007	0.009	1.8
11-HI	-0.005	0.010	1.5
12-HI	-0.012	0.018	2.7

[a] Charges are given in a.u. and energies are in kcal/mol.

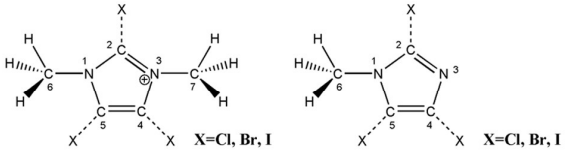

The imidazolium cations **1-6** The imidazole molecules **7-12**

Scheme. 1 The chemical structures of the imidazolium cations **1-6** and the imidazole molecules **7-12**.

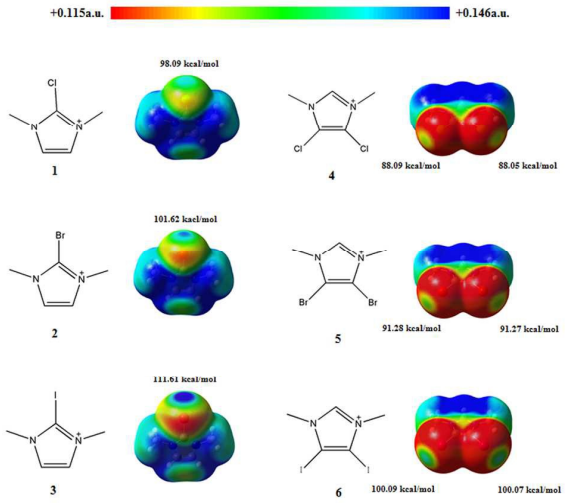

Fig. 1 Electrostatic potential surfaces of the imidazolium cations **1-6**, together with $V_{S,max}$ for X atoms.

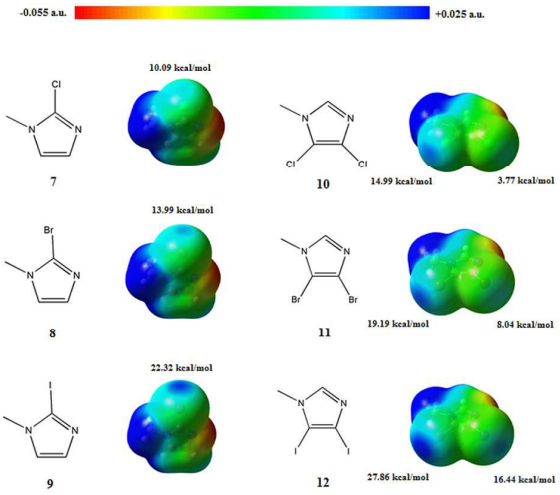

Fig. 2 Electrostatic potential surfaces of the imidazole molecules **7-12**, together with $V_{S,max}$ for X atoms.

RSC Advances

PAPER

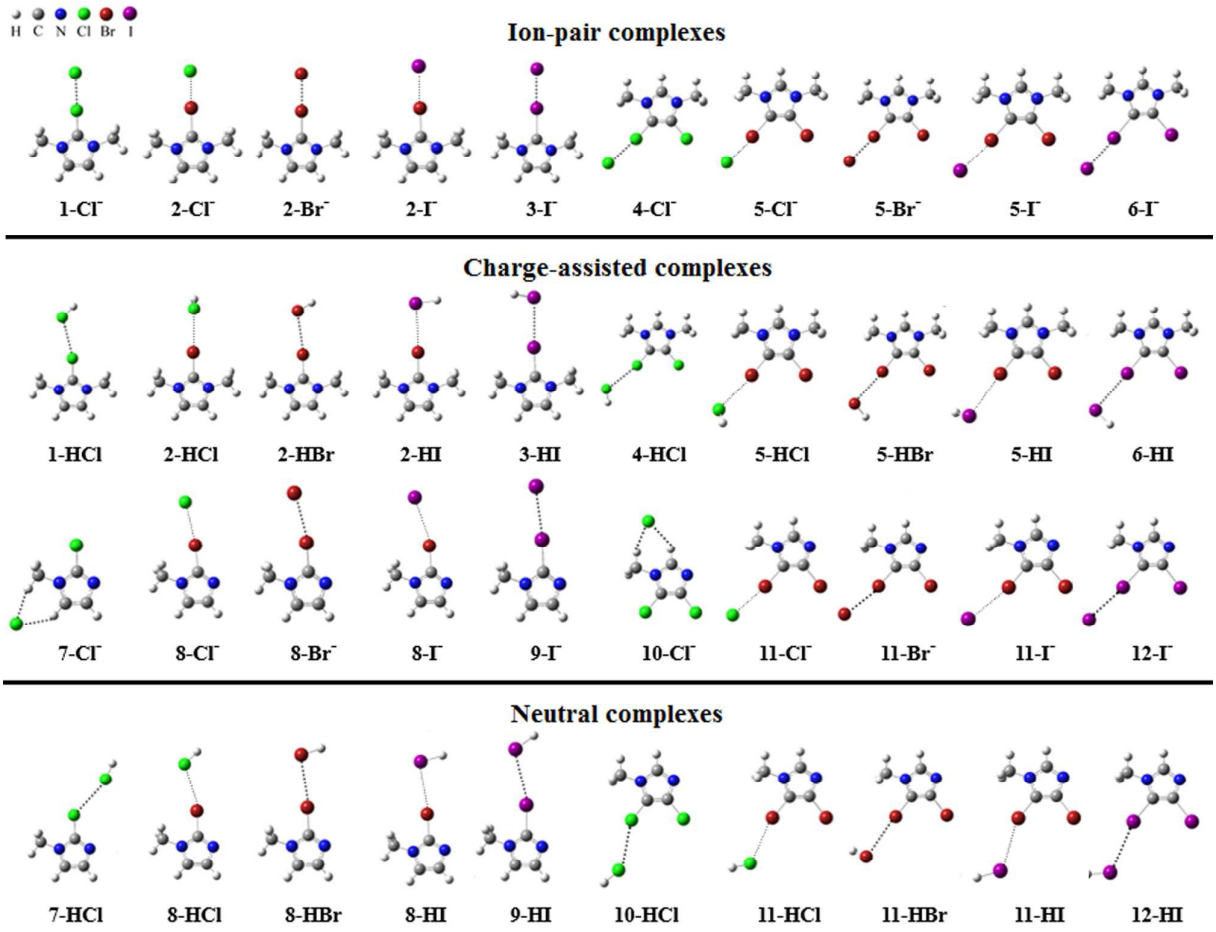

Fig. 3 Optimized structures at the level of M06-2x for the complexes under study.

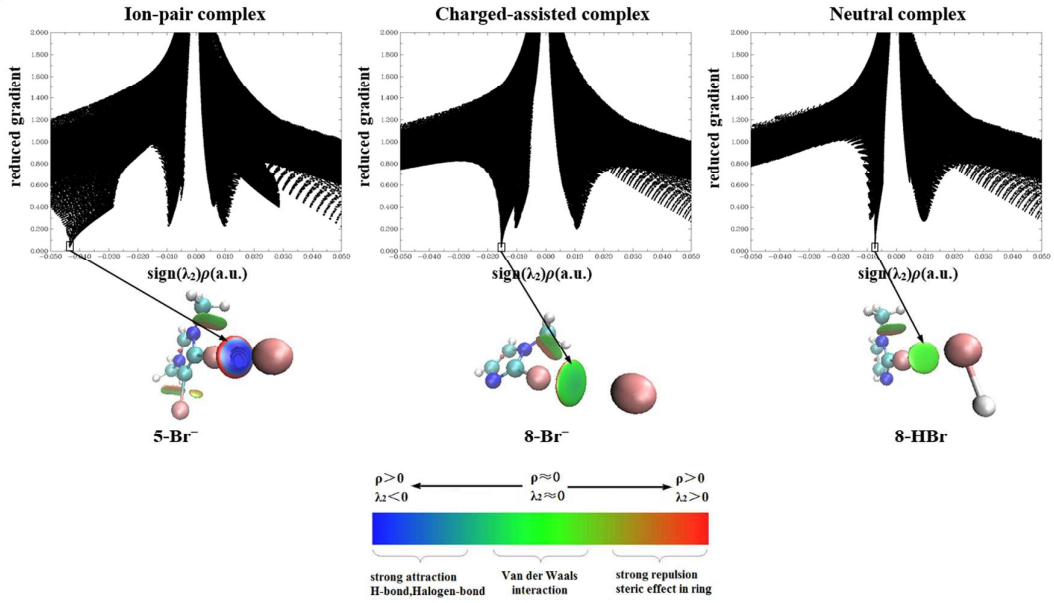

Fig. 4 The NCI isosurfaces and plots of the reduced density gradient versus the electron density multiplied by the sign of the second Hessian eigenvalue for **5**-Br^-, **8**-Br^- and **8**-HBr.

